Effects of Resonant Tesseral Gravity Coefficients on Viking-Type Orbits

HAROLD R. COMPTON* AND JAMES R. SCHIESS†
NASA Langley Research Center, Hampton, Va.
AND
WILLIAM J. BREEDLOVE JR.‡
Old Dominion University, Norfolk, Va.

A special perturbation technique has been developed for the long-period and secular motion of a Viking-type orbiter. The technique uses a method of singly averaging the perturbations over the mean anomaly to determine changes in orbital elements due to atmospheric drag, solar radiation pressure, solar gravity, and the asymmetrical Mars gravitational field. The technique has been specialized to treat resonant tesseral gravity effects resulting from the commensurability of the satellite orbit period with the rotational period of the primary. Results are presented which indicate that orbiter lifetimes can be significantly reduced by resonant tesserals for orbits near the critical inclination. Conversely, it is shown that lifetimes can be extended via capture in resonant orbits which are stable against small drag forces.

Introduction

THE long-term motion of artificial satellites has been discussed extensively in the literature. In the particular case where the satellite mean motion is commensurable with the rotation rate of the primary, the satellite is subject to resonance effects arising from the longitude-dependent terms of the gravity potential. These resonance effects have also received extensive treatment in the literature. For example, Wagner[1,2] discusses the utilization of such motion for geopotential recovery. The utility of such motion results from an accumulation of gravitational perturbations due to the repeated trace of the satellite orbit on the rotating primary. These perturbations are due to certain longitude-dependent potential terms, usually referred to as "resonant tesseral harmonics." It is these terms which are most efficiently determined from resonant orbits. A detailed analytical treatment of the perturbations on low-eccentricity, resonant-satellite orbits with arbitrary inclinations is given by Allan.[3] Allan also treats the case of resonant-satellite orbits with arbitrary eccentricity at critical inclination.[4] This case can be treated analytically because of the near zero rate for the argument of periapsis motion. In Ref. 5 a method of analyzing resonant effects in terms of the so-called stroboscopic mean node is described and the method is applied to a wide spectrum of orbits. Numerous other investigations of resonant-satellite motion are reported in the literature.[6-8] However, none of these is directly applicable to the case of resonant, inclined, and highly elliptical orbits about a planet such as Mars, in the presence of atmospheric drag, solar radiation pressure, solar gravitational perturbations, and asymmetrical gravitational fields. The purpose of this paper is to describe a method for predicting the long-term motion of a spacecraft in such an orbit and to present some of the preliminary results of an application to the Viking Project.

Presented as Paper 73-143 at the AIAA 11th Aerospace Science Meeting, Washington D.C., January 10–12, 1973; submitted March 26, 1973; revision received August 6, 1973.
Index category: Navigation, Control, and Guidance Theory.

* Aerospace Technologist, Lunar and Planetary Sciences Section, Planetary Physics Branch, Environmental and Space Sciences Division.
† Aerospace Technologist, Flight Applications Section, Computer Mathematics and Programing Branch, Analysis and Computations Division.
‡ Assistant Professor of Engineering. Associate Member AIAA.

The Viking Project calls for two orbiting spacecraft to conduct scientific surveillance of the planet Mars in conjunction with two landed spacecraft.[9] The two orbiting spacecraft will have orbital periods nearly commensurate with the Mars rotational period and will be in inclined and highly elliptical ($e > 0.7$) orbits. The ephemerides of these two spacecraft will be determined in real time through the use of radio Doppler tracking data in conjunction with orbit determination and prediction techniques. Generally, the orbit prediction technique treats all possible terms (short periodic, long periodic, and secular) in the satellite theory. However, for long-term orbit prediction and lifetime studies only the long-period and secular terms in the satellite theory are considered. Normally, such a method operates much faster on the computer and affords considerable savings in computer time and money. This method also lends itself to more efficient determination of certain gravitational coefficients.

A special perturbation technique for the long-period and secular motion of a Mars orbiter has been developed.[10] The technique uses a method of singly averaging the perturbations over the mean anomaly to determine changes in orbital elements due to atmospheric drag, solar radiation pressure, solar gravity, and the asymmetrical Mars gravitational field. The method is similar to that reported in Ref. 11 for Earth orbits as far as the treatment of the tesseral harmonics and solar perturbations is concerned. In addition, however, the effects of solar radiation pressure and drag based on a time-varying exponential atmosphere are included. This is a requirement since the atmospheric density of Mars varies by at least two orders of magnitude between maximum and minimum solar activity.

Equations of Motion

The equations of motion of the orbiter are the Lagrange Planetary Equations with appropriate additions to the right-hand side to account for atmospheric drag and solar radiation pressure. These equations may be written in matrix form in terms of the Keplerian orbital elements as

$$\dot{C} = \Phi DR + GF \tag{1}$$

where

$$C^T = [a\ e\ i\ \Omega\ \omega\ M]$$

$$D^T = [(\partial/\partial a)(\partial/\partial e)(\partial/\partial i)(\partial/\partial\Omega)(\partial/\partial\omega)(\partial/\partial M)]$$

$$\Phi \equiv \text{"Poisson Matrix"} \equiv \Phi(a, e, i, \Omega, \omega, M)$$

Table 1 Elements of Φ and G matrix

$\Phi_{16} = [2/na]$; $\Phi_{25} = -[(1-e^2)^{1/2}/na^2e]$; $\Phi_{26} = [(1-e^2)/na^2e]$;
$\Phi_{34} = -[csci/na^2(1-e^2)^{1/2}]$; $\Phi_{35} = [\cot i/na^2(1-e^2)^{1/2}]$;
$\Phi_{43} = [1/na^2(1-e^2)^{1/2}\sin i]$; $\Phi_{52} = [(1-e^2)^{1/2}/na^2e]$;
$\Phi_{53} = [-\cot i/na^2(1-e^2)^{1/2}]$;
$\Phi_{61} = -[2/na]$; $\Phi_{62} = -[(1-e^2)/na^2e]$.
$G_{11} = [2e\sin f/n(1-e^2)^{1/2}]$; $G_{12} = [2a(1-e^2)^{1/2}/nr]$;
$G_{21} = [(1-e^2)^{1/2}\sin f/na]$;
$G_{22} = [(\{1-e^2\}^{1/2}/na^2e)(a^2\{1-e^2\}/r-r)]$;
$G_{33} = [r\cos\omega/na^2(1-e^2)^{1/2}]$;
$G_{43} = [r\sin\omega/na^2(1-e^2)^{1/2}\sin i]$; $G_{51} = -[(1-e^2)^{1/2}\cos f/nae]$;
$G_{52} = [\{(1-e^2)^{1/2}\sin f/nae\}\{1+r/a(1-e^2)\}]$;
$G_{53} = -[r\sin\omega\cot i/na^2(1-e^2)^{1/2}]$;
$G_{61} = -[(\mu a)^{-1/2}\{2r-a(1-e^2)\cos f/e\}]$;
$G_{62} = -[(\mu a)^{-1/2}\{r+a(1-e^2)\}\sin f/e]$.

G = Matrix stemming from Gaussian form of planetary equations

$R \equiv R_{\sigma} + R_{\odot} \equiv$ Mars and solar gravity potential

F = Vector of atmospheric drag and solar radiation pressure forces

The superscript T denotes the matrix transpose and the dot ($\dot{C}$) indicates a derivative with respect to time. The Keplerian elements, a, e, i, Ω, ω, and M are, respectively, the semimajor axis, eccentricity, inclination, longitude of the node, argument of periapsis, and mean anomaly of the orbit. The nonzero elements of the Φ and G matrices are given in Table 1.

The components of the vector F are mutually orthogonal and consist of forces due to the atmospheric drag and solar radiation pressure. The drag model is that given by Fitzpatrick[12] and assumes a neutral spherically symmetric and rotating (constant angular rate) atmosphere. The solar radiation pressure model is the same as that given by Shapiro in Ref. 13.

The disturbing function R is composed of the Mars gravity potential, R_{σ}, and the solar gravity potential, $R_{\odot}$. The functions R_{σ} and $R_{\odot}$ are given by Kaula in Refs. 6 and 14, respectively.

A detailed discussion of the equations of motion and their solution as used in this paper is given in Ref. 10. However, it should be noted that Eqs. (1) are given in terms of osculating orbital elements and the usual approach is to average the right-hand side to obtain the long-period and secular motion.

In general, the averaging of Eqs. (1) is straightforward; however, for Viking-type orbits, that portion of the disturbing function due to the Mars gravity potential must receive special attention because of resonance. First, consider Eqs. (1) in the symbolic averaged form

$$\dot{\bar{C}} = \frac{1}{2\pi}\int_0^{2\pi}[\Phi DR + GF]\,dM$$
$$= \frac{1}{2\pi}\int_0^{2\pi}[\Phi DR_{\sigma}]\,dM + \frac{1}{2\pi}\int_0^{2\pi}[\Phi DR_{\odot}]\,dM + \frac{1}{2\pi}\int_0^{2\pi}[GF_D]\,dM + \frac{1}{2\pi}\int_0^{2\pi}[GF_{\odot}]\,dM \qquad (2)$$

where F_D and $F_{\odot}$, respectively, are the forces due to atmospheric drag and solar radiation pressure, and barred quantities refer to averaged values.

Kaula[14] has derived the disturbing function of the sun, $R_{\odot}$, as that due to a point mass acting on a satellite in terms of the planet-centered elements of the sun and the satellite. The general form of the solar disturbing function after averaging is

$$\bar{R}_{\odot} = m_{\odot}\sum_{n=2}^{\infty}\sum_{m=0}^{n}\sum_{p=0}^{n}\sum_{h=0}^{n}\sum_{j=-\infty}^{\infty} R(\omega,\Omega,a,i,e,\omega_s,\Omega_s,a_s,i_s,e_s,M_s)_{nmphqj}$$

where the subscript s denotes the Mars-centered sun elements and $m_{\odot}$ is the mass of the sun. For practical applications, the summations over n and j may be restricted to a few terms.

The solar radiation pressure model assumes a spherical spacecraft impacted by parallel solar rays. Shadow effects are incorporated in the model. The effects of the solar radiation pressure on the orbiter are calculated by first averaging analytically the effect over one orbital period. A pro-rated increment, based on the integration step-size used for integrating Lagrange's equations, is then added to the elements after each step in the integration procedure.

The atmospheric drag model employed is the one presented by Fitzpatrick in Ref. 12. The atmosphere is assumed to be spherically symmetrical and rotating with a constant rate. Furthermore, the atmospheric density can be treated as either a time-varying or constant exponential. The averaging of the atmospheric drag term is accomplished numerically over one orbital period using a Gaussian quadrature scheme. A pro-rated increment is then added to the elements after each integration step. The averaging is done numerically rather than analytically because of the assumed rotation of the atmosphere.

For convenience of use, Kaula[6] has transformed the gravity potential of any primary expressed in terms of spherical coordinates into a form which is a function of orbital elements. This is the form of R_{σ} as used in this paper and is repeated here as

$$R_{\sigma} = \frac{\mu}{2a} + \sum_{l=2}^{\infty}\sum_{m=0}^{l}\sum_{p=0}^{l}\sum_{q=-\infty}^{\infty} R_{lmpq}$$

where for a given l, m, p, and q

$$R_{lmpq} = \frac{\mu a_e^{\,l}}{a^{l+1}} F(i)_{lmp}\, G(e)_{lpq}\, S_{lmpq}$$

with

$$S_{lmpq} = \begin{bmatrix} C_{lm} \\ -S_{lm} \end{bmatrix}^{\text{even}}_{\text{odd}}{}^{l-m}_{l-m} \cos\Psi_{lmpq} + \begin{bmatrix} S_{lm} \\ C_{lm} \end{bmatrix}^{\text{even}}_{\text{odd}}{}^{l-m}_{l-m} \sin\Psi_{lmpq}$$

and

$$\Psi_{lmpq} = [(l-2p)\omega + (l-2p+q)M + m(\Omega-\Theta)]$$

The terms C_{lm} and S_{lm} are the coefficients in the expansion of the potential in terms of spherical harmonics where l and m are, respectively, the degree and order of the associated Legendre polynomials. The mean radius of Mars is denoted by a_e and μ is the product of the universal gravitational constant and the mass of Mars. The F and G functions are given in detail in Ref. 6, and p and q are indices of summations. The angle Θ is defined by the equation

$$\Theta = \Theta_0 + \dot{\Theta}t$$

where $\dot{\Theta}$ is the rotational rate of the primary (Mars) and t is time.

Usually the averaging of R_{σ} is accomplished by integration of the function over the mean anomaly and division by 2π.

$$\bar{R}_{\sigma} = \frac{1}{2\pi}\int_0^{2\pi} R_{\sigma}\,dM$$

It is normally assumed that all orbital elements are constant over the interval of integration. The equivalent of this averaging is obtained by setting $l-2p+q=0$ in R_{σ}. However, for this case the averaging process is not straightforward because of the existence of two fast variables, M and Θ, in R_{σ}. For Viking-type orbits, $\dot{M} \approx \dot{\Theta}$, and the existence of both M and Θ in the potential function requires that the function be doubly averaged. This not only produces mathematical problems in forming the averages but also noticeable long-period perturbations in the orbital elements due to certain tesseral gravity coefficients, which in this case are no longer short periodic terms. This phenomena is referred to as tesseral resonance and occurs when the period of the satellite orbit is commensurate with the rotational period of the primary.

An integration of R_{σ} cannot be made independently over first M and then Θ since a constraint of the form $\dot{M} \approx \dot{\Theta}$ exists over the integration interval where $\dot{M}$ is the mean motion

defined by $(\mu/a^3)^{1/2}$. To avoid the double averaging problem, a new variable[5] is introduced as

$$\lambda = (\Omega - \Theta) + \kappa(M + \omega)$$

and is used to eliminate Θ from the potential function so that

$$R_{\mathcal{J}} = R_{\mathcal{J}}\ (a, e, i, \Omega, \omega, M, \lambda)$$

κ is chosen so that λ is a slowly-varying angle variable and is defined as

$$\kappa = (r/s) + \Delta$$

where r and s are relatively prime integers and $0 \leqq \Delta < 1$. For $\Delta = 0$, exact resonance exists. For Viking-type orbits, $r/s \approx 1$. The potential, $R_{\mathcal{J}}$, is now a function of only one fast variable, M, and hence averaging can proceed in the usual manner.

The new variable changes the form of the arguments of the trigonometric functions in $R_{\mathcal{J}}$ and consequently the form of the partial derivatives used on the right-hand side of Eqs. (2). The argument now becomes

$$\Psi_{lmpq} = [m\lambda + (l - 2p - \kappa m)\omega + (l - 2p + q - \kappa m)M]$$

With this new form of the argument, $R_{\mathcal{J}}$ can be considered as the sum of three separate terms.

$$R_{\mathcal{J}} = R_{\mathcal{J}}\Big|_{\substack{m=0 \\ l-2p+q\neq 0}} + R_{\mathcal{J}}\Big|_{\substack{m=0 \\ l-2p+q=0}} + R_{\mathcal{J}}\Big|_{\text{all remaining terms}} \equiv R^{(1)} + R^{(2)} + R^{(\text{art})}$$

If $R_{\mathcal{J}}$ is averaged over the mean anomaly, the following expressions are obtained:

$$\bar{R}_{\mathcal{J}} = \bar{R}^{(1)} + \bar{R}^{(2)} + \bar{R}^{(\text{art})}$$

and

$$\bar{R}^{(1)} = 0$$

$$\bar{R}^{(2)} = \sum_{l=2}^{\infty} \sum_{p=0}^{l} \frac{\mu a_e^{\,l}}{a^{l+1}} F_{l0p} G_{lp(2p-l)} S_{l0(2p-l)}$$

$$\bar{R}^{(\text{art})} = \frac{1}{2\pi} \sum_{l=2}^{\infty} \sum_{m=0}^{l} \sum_{p=0}^{l} \sum_{q=-\infty}^{\infty} \frac{\mu a_e^{\,l}}{a^{l+1}} F_{lmp} G_{lpq*} \hat{S}_{lmpq*}$$

where

$$\hat{S} = \frac{1}{l - 2p + q - \kappa m} \left[S'_{lmpq*} \right]_{M=0}^{M=2\pi}$$

and S' indicates the integrated form of S_{lmpq}. The asterisk here indicates that all terms with $m = 0$ are to be omitted. The denominator of $\hat{S}$ may be written as

$$\delta = l - 2p + q - (r/s)m - m\Delta$$

When $l - 2p + q = (r/s)m$, and $\Delta = 0$, as in the case for exact resonance, a zero denominator appears in the expression for $\bar{R}^{(\text{art})}$. Theoretically, a finite limit of this function exists, but numerically, the small divisors may present problems. The gravity coefficients characterized by

$$l - 2p + q = (r/s)m$$

are called the "resonant tesserals" and it is these terms which "resonate" with the particular orbit and produce significant long-period effects. For orbits having the same period as the rotation of the primary, $r/s = 1$, and all tesseral coefficients are resonant.

In order to avoid the numerical difficulty that arises from small divisors, a resonant averaged disturbing function can be constructed by further defining

$$R^{(\text{art})} = R\Big|_{\substack{m\neq 0 \\ m(r/s)=\text{integer} \\ l-2p+q\neq m(r/s)}} + R\Big|_{\substack{m\neq 0 \\ m(r/s)=\text{integer} \\ m(r/s)=l-2p+q}} + R\Big|_{\substack{m\neq 0 \\ m(r/s)\neq\text{integer}}}$$

and

$$\bar{R}^{(\text{art})} = \bar{R}^{(3)} + \bar{R}^{(4)} + \bar{R}^{(5)}$$

where

$$\bar{R}^{(3)} = 0$$

$$\bar{R}^{(4)} = \sum_{l=2}^{\infty} \sum_{m=0}^{l} \sum_{p=0}^{l} \frac{\mu a_e^{\,l}}{a^{l+1}} F_{lmp} G_{lp\gamma} S_{lmp\gamma}$$

$$\bar{R}^{(5)} = \frac{1}{2\pi} \sum_{l=2}^{\infty} \sum_{m=0}^{l} \sum_{p=0}^{l} \sum_{q=-\infty}^{\infty} \frac{\mu a_e^{\,l}}{a^{l+1}} F_{lmp} G_{lpq*} \hat{S}_{lmpq*}$$

$$\hat{S} = \frac{1}{[l - 2p + q - (r/s)m]} \left[S'_{lmpq} \right]_{M=0}^{M=2\pi}$$

and where the asterisk indicates that terms already included in $\bar{R}^{(3)}$ and $\bar{R}^{(4)}$ are to be omitted from the summation and $\gamma = [2p - l + (r/s)m]$.

For resonant orbits, the terms in $\bar{R}^{(5)}$ produce periodic perturbations with periods much smaller than those due to $\bar{R}^{(4)}$. Thus $\bar{R}^{(5)}$ has been omitted and the averaged disturbing function is given as

$$\bar{R}_{\mathcal{J}} = \bar{R}^{(2)} + \bar{R}^{(4)}$$

This is the function that has been substituted on the right-hand side of Lagrange's equation to obtain the long-period and secular rates of the orbital elements. These rates are then integrated numerically to obtain the long-term motion of the orbiter.

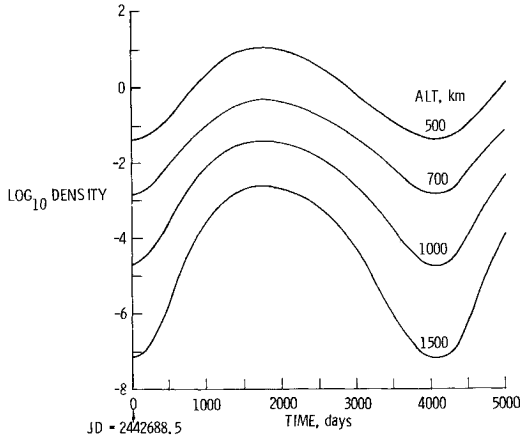

Fig. 1 Mars atmospheric density (kg/km^3) variation with time at constant altitudes.

Application to a Viking-Type Orbiter

The equations of motion have been programed for the CDC-6600 digital computer. The program has been utilized to obtain the long-term motion of a synchronous Mars orbiter of the type planned in the Viking Project. Particular attention has been given to orbital lifetimes since Viking planetary quarantine (PQ) restrictions require a 42-yr orbiter lifetime. In particular, the effects of the resonant tesseral gravity coefficients, $C_{2,2}$ and $S_{2,2}$ in addition to $C_{2,0}$ have been studied. These coefficients are expected to be the dominant ones, and at this time are the only ones for which we have reliable values.[15] The basic approach has been to model the dynamics using solar radiation pressure, atmospheric drag, solar gravitational perturbations, and the Mars gravitational field.

The time-varying atmospheric density profile used in the drag model is shown in Fig. 1 for several different altitudes. At the lower altitudes, the density variation from a solar maximum to a solar minimum is about two orders of magnitude and at the higher altitude is about four orders of magnitude. The effective cross sectional area used for both drag and solar radiation pressure was 19.4 m^2.

The characteristics of the nominal orbit used in this analysis are given in Table 2. The angles are referenced to the Mars equator and equinox for the epoch date shown. The large values of semimajor axis, eccentricity, and inclination, and the synchronous orbit period are typical of those being considered for the Viking orbiter. The values used for the gravity coefficients are also given in Table 2.

Table 2 Nominal orbit parameters and gravity coefficients

Orbit parameters	Gravity coefficient
$a = 20427.71$ km $e = 0.7604528$ $i = 45.0°$ $\Omega = 88.77°$ $\omega = 57.64°$ $h_p = 1500$ km period = 24.623 hr Epoch date = 2443056.0 JD	$C_{2,0} = -1.97 \times 10^{-3}$ $C_{2,2} = -5 \times 10^{-5}$ $S_{2,2} = 3 \times 10^{-5}$

Perhaps the most interesting motion encountered in these preliminary analyses was that of synchronous orbital capture in the presence of atmospheric drag. It was found that a Viking-type orbiter, with a small atmospheric drag acting on it, could remain in a synchronous or near-synchronous orbit for long periods of time, and that the period of the orbit oscillated about the synchronous values. This behavior is due to orbiter resonance with the tesseral harmonics. The orbiter gains enough energy each revolution to counteract the energy loss due to drag. The possibility of such a motion was predicted by R. R. Allan in Ref. 3 for low-eccentricity orbits. An example of this resonance-type of motion is given in Fig. 2 where the time history of the orbital elements and the periapsis altitude for the nominal orbit are shown for a period of 2000 days. The element variations are given with and without the use of $C_{2,2}$ and $S_{2,2}$. Without the tesserals, the semimajor axis decays slowly due to drag as might be expected. However, with the tesserals included, the orbiter remains in a synchronous resonant orbit, that is, the semimajor axis and the orbital period oscillate (period approximately 150 days) around the synchronous values for the entire time span shown. This observation may not be significant for satellites at this altitude since the lifetime would be very long even in the absence of resonance, but it does suggest the possibility of extended lifetimes via resonant capture orbits at lower altitudes where drag effects are much larger.

Variations of this phenomena were encountered at the lower periapsis altitudes. An example of this phenomena is given in Fig. 3 where the time history of the nominal orbit elements is given for an initial value of periapsis altitude of 700 km. Here the orbit remained nearly synchronous for about 1100 days and then decayed rapidly due to the increasing dominance of the drag forces. The onset of rapid decay corresponds nearly to the point of maximum density shown in Fig. 1. The important point is that even though the drag was dominant in the end, the resonant tesserals preserved the synchronous conditions over an extended period of time. This again suggests the possibility of extended lifetimes via resonant capture orbits.

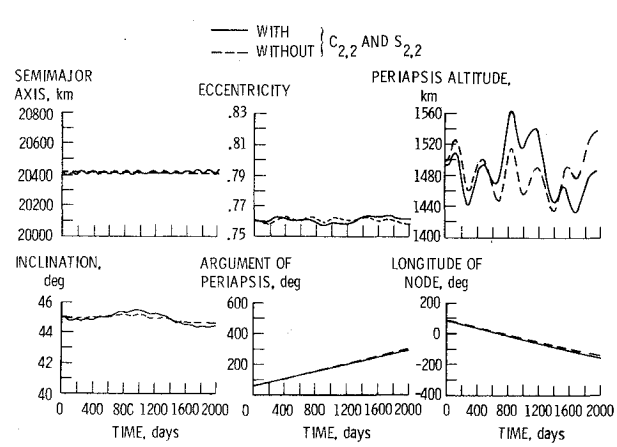

Fig. 2 Variation of orbital elements with time for initial periapsis altitude of 1500 km. (With and without $C_{2,2}$ and $S_{2,2}$).

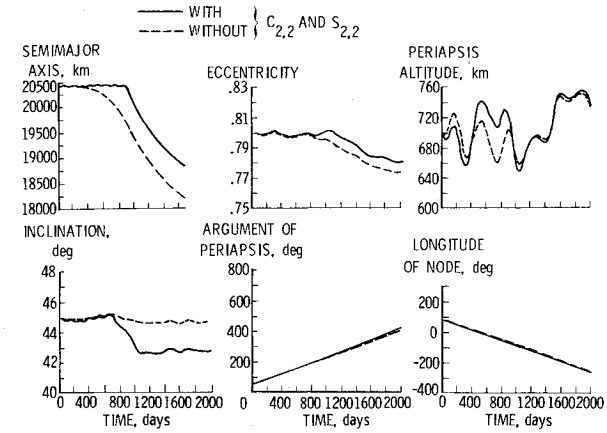

Fig. 3 Variation of orbital elements with time for initial periapsis altitude of 700 km. (With and without $C_{2,2}$ and $S_{2,2}$).

Some preliminary investigations suggested the possibility that the capture phenomena might be a strong function of the inclination. To investigate this further, the inclination was varied between 5° and 90° with initial periapsis altitudes of 700 and 1500 km. Some representative results of this variation are shown in Figs. 4–6 where the time variation of the semimajor axis, eccentricity, and periapsis altitude is given for an initial periapsis altitude of 700 km. Notice in Fig. 4 that as the inclination increases from the lower values to a point near the critical value (63.4°) the onset of orbit decay occurs much earlier. After passage through critical inclination, the resonant capture phenomena is again extended to longer time periods. Thus, tesseral resonant effects can significantly change orbital lifetimes, and maximum decay and minimum capture time due to these tesserals occur near the critical inclination. For initial periapsis altitude of 1500 km, the orbiter remained in resonance for all values of inclination investigated.

It is evident from Figs. 2–7 that under certain conditions $C_{2,2}$ and $S_{2,2}$ produce significant periodic and secular variations in the orbit eccentricity and semimajor axis and consequently in the periapsis altitude. It is also evident from Figs. 6 and 7 that the effects of resonant tesserals on the periapsis altitude are strongly dependent on the inclination and that the maximum effects occur in the vicinity of the critical inclination. For example, in Fig. 7 at an inclination of 65° the periapsis altitude after 2000 days is 250 km lower than that calculated without $C_{2,2}$ and $S_{2,2}$. Also, the difference between the two curves appears to be increasing secularly in a direction of lower periapsis altitudes indicating that in the long run the satellite lifetime

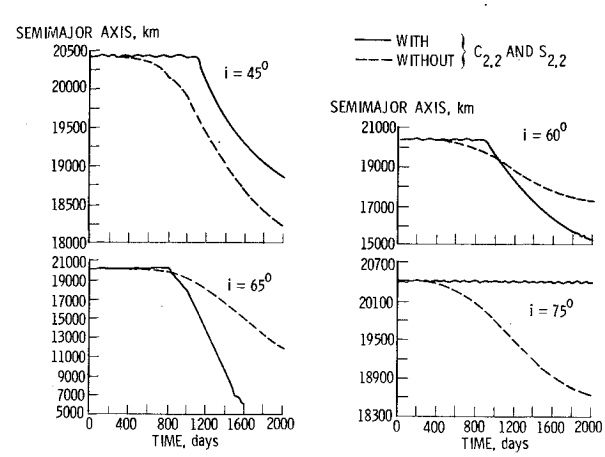

Fig. 4 Variation of semimajor axis with time at inclinations of 45°, 60°, 65°, and 75° for initial periapsis altitude of 700 km. (With and without $C_{2,2}$ and $S_{2,2}$).

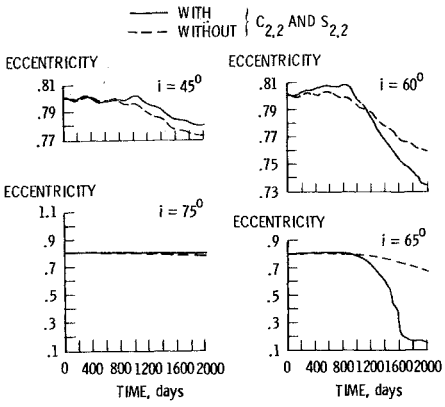

Fig. 5 Variation of eccentricity with time at inclinations of 45°, 60°, 65°, and 75° for initial periapsis altitude of 700 km. (With and without $C_{2,2}$ and $S_{2,2}$).

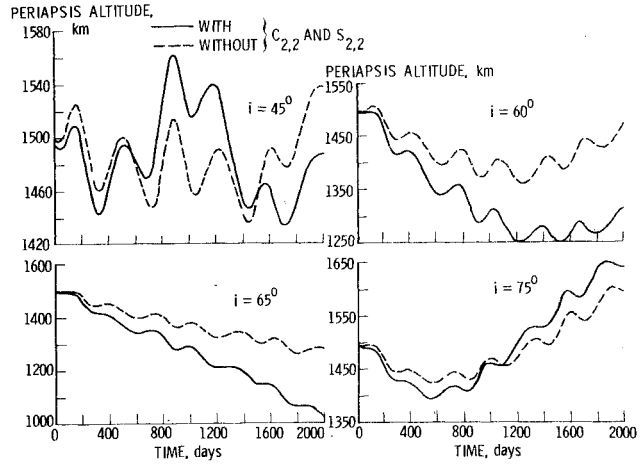

Fig. 7 Variation of periapsis altitude with time at inclinations of 45°, 60°, 65°, and 75° for initial periapsis altitude of 1500 km. (With and without $C_{2,2}$ and $S_{2,2}$).

may be in jeopardy. For inclinations sufficiently different (approximately 10°) from the critical value, the dispersion in periapsis altitude due to the tesseral harmonics is not nearly so large. Similar results were noted at the lower initial periapsis altitude. The point to be made here is that tesseral coefficients can cause significant changes in periapsis altitudes; especially in the vicinity of critical inclination, and from the standpoint of *PQ* restrictions, orbits requiring inclinations near the critical value should receive careful analysis. In fact, the results obtained so far indicate that, for the nominal orbit at critical inclination, the minimum allowable initial periapsis altitude for a 42-yr lifetime is about 1700 km.

Allan[3] has shown that very low eccentricity resonant orbits undergo a secular decrease in orbit inclination. Similar results were noted in this analysis for orbits with high eccentricity (Fig. 3). This effect seems to be most prevalent at the higher inclinations and lower periapsis altitudes.

The resonant tesseral effects on orbital lifetime were also found to be very dependent upon the argument of periapsis, ω. In order to examine this effect, the argument of periapsis was varied between 0° and 180°. An inclination of 65° was chosen since orbit lifetime perturbations were largest in the vicinity of critical inclination. In each case it was found that inclusion of $C_{2,2}$ and $S_{2,2}$ in the Mars potential resulted in an oscillation of the semimajor axis about the synchronous orbit value with a maximum amplitude of about 10 km. Without these two coefficients, the semimajor axis decayed slowly as expected, with the maximum decay after 11 years being only about 50 km. The variations in periapsis altitude for these conditions are shown in Fig. 8 for a period of about 4200 days for five different values of ω. This time interval is equivalent to one solar cycle, and thus allows the evolution of the orbit over one complete cycle of the drag density curve. The variations are both periodic and secular; however, it appears that the major effect of the tesserals is a change in the secular rates. The dependence of these variations on the magnitude of the argument of periapsis is consistent with the analysis presented by Gedeon[16] for critically inclined orbits. The importance of this effect is in the resulting orbital lifetime variations. For example, for ω equal to 90° there is a difference of periapsis altitude of 800 km after about 4200 days. It appears that this difference will continue to increase. Also, note that after about 3000 days the periapsis altitude for ω equal to 135° with tesserals included begins to decrease very rapidly so that after 4200 days it differs from that without the tesserals by approximately 600 km. There have been some indications that maximum periapsis decrease as a function of ω is dependent on the orbit inclination. However, it appears that the maximum effect in terms of lifetime considerations is near critical inclination with ω equal to 90° or 135°.

Conclusions

A special perturbation technique has been developed to predict the long-period and secular motion of a Viking-type orbiter.

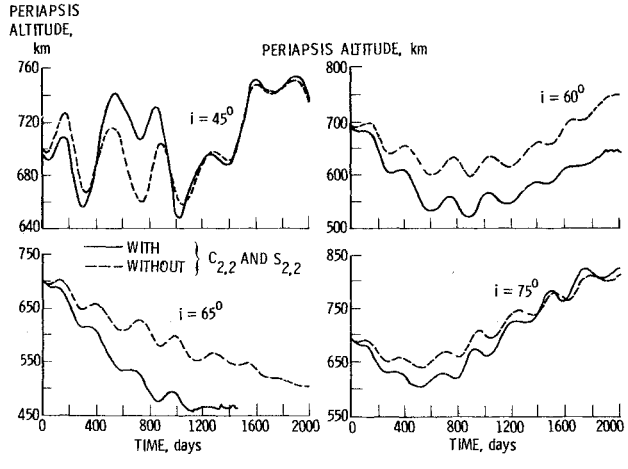

Fig. 6 Variation of periapsis altitude with time at inclinations of 45°, 60°, 65°, and 75° for initial periapsis altitude of 700 km. (With and without $C_{2,2}$ and $S_{2,2}$).

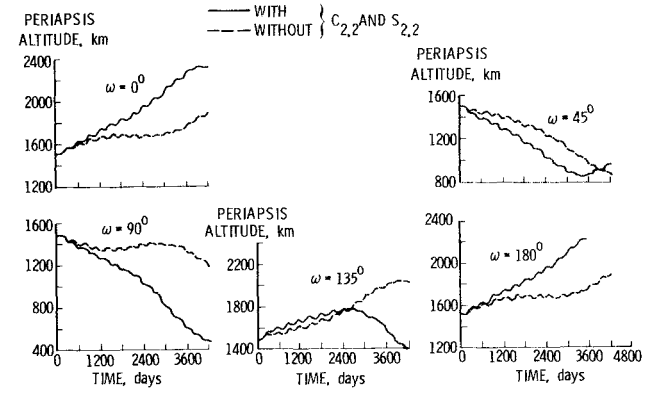

Fig. 8 Variation of periapsis altitude with time at argument of periapsis of 0°, 45°, 90°, 135°, 180° for initial periapsis altitude of 1500 km. (With and without $C_{2,2}$ and $S_{2,2}$).

The technique was specialized to treat resonant tesseral gravity effects resulting from the commensurability of the satellite orbit period with the rotational period of the primary. In addition, the effects of solar radiation pressure, solar gravity, and atmospheric drag were considered. The technique was applied to a typical Viking-type orbit and it was found that this type of orbit could be stable against small drag forces for an extended period of time. The preliminary results indicate that orbit lifetimes for orbits near the critical inclination can be significantly reduced by the resonant tesseral gravity coefficients $C_{2,2}$ and $S_{2,2}$. A secular decrease in the orbital inclination was noted during stable resonance. It was found that resonant tesseral effects on orbit lifetime are very dependent upon the argument of periapsis. For near critical inclination orbits, the maximum effect occurred for ω equal to 90° and 135°.

References

[1] Wagner, C. A., "Geopotential Coefficients Recovery from Very Long Arcs of Resonant Orbits," *Journal of Geophysical Research*, Vol. 75, No. 32, 1970, pp. 6662–6674.

[2] Wagner, C. A., "Combined Solution for Low Degree Longitude Harmonics of Gravity from 12- and 24-Hour Satellites," *Journal of Geophysical Research*, Vol. 73, 1968, pp. 7651–7659.

[3] Allan, R. R., "Resonance Effects Due to the Longitude Dependence of the Gravitational Field of a Rotating Primary," Royal Aircraft Establishment TR 66279, Aug. 1966, Ministry of Aviation, Farnborough, Hants, England.

[4] Allan, R. R., "Commensurable Eccentric Orbits near Critical Inclination," *Celestial Mechanics*, Vol. 3, 1971, pp. 320–330.

[5] Gedeon, G. S., "Tesseral Resonance Effects on Satellite Orbits," *Celestial Mechanics*, Vol. 1, 1969, pp. 167–189.

[6] Kaula, W. M., *Theory of Satellite Geodesy*, Blaisdell Publishing Co., Waltham, Mass., 1966.

[7] Garfinkel, B., "Comparison of the Classical and the Global Solutions of the Ideal Resonance Problem," *Celestial Mechanics*, Vol. 5, 1972, p. 451.

[8] Douglas, B. C. and Palmiter, M. T., "An Analysis of Eccentric Deeply Resonant Orbits for Geodesy," *Astronautical Sciences*, Vol. 17, No. 6, 1970, pp. 313–336.

[9] Viking Project Management, "1973 Viking Voyage to Mars," *Aeronautics & Astronautics*, Vol. 7, No. 11, 1969, pp. 30–59.

[10] Breedlove, W. J., "Determination of the Atmospheric and Gravitational Parameters of Mars from a Study of the Long-Period Motion of a Viking Orbiter," Final Rept. NAS1-9434-44, 1972, Old Dominion Univ. Research Foundation, Norfolk, Va.

[11] Wagner, C. A., Douglas, B. C., and Fisher, E. R., "Resonant Satellite Geodesy by High Speed Analysis of Mean Kepler Elements," TM X-63586, 1969, NASA.

[12] Fitzpatrick, P. M., *Principles of Celestial Mechanics*, Academic Press, New York, 1970.

[13] Shapiro, I. I., "The Prediction of Satellite Orbits," *Dynamics of Satellites*, Proceedings of IUTAM Paris Conference, May 1962, Academic Press, New York, 1963.

[14] Kaula, W. M., "Development of the Lunar and Solar Disturbing Functions for a Close Satellite," *Astronomical Journal*, Vol. 67, No. 5, 1962, p. 300.

[15] Lorell, J. et al., "Mariner 9 Celestial Mechanics Experiment: Gravity Field and Pole Direction of Mars," *Science*, Vol. 175, No. 4019, Jan. 1972, pp. 317–320.

[16] Gedeon, G. S., Douglas, B. C., and Palmiter, M. T., "Resonance Effects on Eccentric Satellite Orbits," *The Journal of the Astronautical Sciences*, Vol. XIV, No. 4, 1967, pp. 147–157.